Design, Synthesis, and Antifolate Activity of New Analogues of Piritrexim and Other Diaminopyrimidine Dihydrofolate Reductase Inhibitors with ω-Carboxyalkoxy or ω-Carboxy-1-alkynyl...

ARTICLE *in* JOURNAL OF MEDICINAL CHEMISTRY · JULY 2005

Impact Factor: 5.45 · DOI: 10.1021/jm0581718 · Source: PubMed

5 AUTHORS, INCLUDING:

Sherry F Queener
Indiana University-Purdue University Indiana...
226 PUBLICATIONS **4,794** CITATIONS
SEE PROFILE

Andre Rosowsky
Dana-Farber Cancer Institute
292 PUBLICATIONS **5,469** CITATIONS
SEE PROFILE

Design, Synthesis, and Antifolate Activity of New Analogues of Piritrexim and Other Diaminopyrimidine Dihydrofolate Reductase Inhibitors with ω-Carboxyalkoxy or ω-Carboxy-1-alkynyl Substitution in the Side Chain

David C. M. Chan,[†] Hongning Fu,[†] Ronald A. Forsch,[†] Sherry F. Queener,[‡] and Andre Rosowsky*,[†]

Dana-Farber Cancer Institute and Department of Biological Chemistry and Molecular Pharmacology, Harvard Medical School, Boston, Massachusetts 02115, and Department of Pharmacology and Toxicology, Indiana University School of Medicine, Indianapolis, Indiana 46202

Received January 19, 2005

As part of a search for dihydrofolate reductase (DHFR) inhibitors combining the high potency of piritrexim (PTX) with the high antiparasitic vs mammalian selectivity of trimethoprim (TMP), the heretofore undescribed 2,4-diamino-6-(2′,5′-disubstituted benzyl)pyrido[2,3-*d*]pyrimidines **6**−**14** with *O*-(ω-carboxyalkyl) or ω-carboxy-1-alkynyl groups on the benzyl moiety were synthesized and tested against *Pneumocystis carinii*, *Toxoplasma gondii*, and *Mycobacterium avium* DHFR vs rat DHFR. Three *N*-(2,4-diaminopteridin-6-yl)methyl)-2′-(ω-carboxy-1-alkynyl)-dibenz[*b*,*f*]azepines (**19**-**21**) were also synthesized and tested. The pyridopyrimidine with the best combination of potency and selectivity was 2,4-diamino-5-methyl-6-[2′-(5-carboxy-1-butynyl)-5′-methoxy]benzyl]pyrimidine (**13**), with an IC_{50} value of 0.65 nM against *P. carinii* DHFR, 0.57 nM against *M. avium* DHFR, and 55 nM against rat DHFR. The potency of **13** against *P. carinii* DHFR was 20-fold greater than that of PTX (IC_{50} = 13 nM), and its selectivity index (SI) relative to rat DHFR was 85, whereas PTX was nonselective. The activity of **13** against *P. carinii* DHFR was 20 000 times greater than that of TMP, with an SI of 96, whereas that of TMP was only 14. However **13** was no more potent than PTX against *M. avium* DHFR, and its SI was no better than that of TMP. Molecular modeling dynamics studies using compounds **10** and **13** indicated a slight binding preference for the latter, in qualitative agreement with the IC_{50} data. Among the pteridines, the most potent against *P. carinii* DHFR and *M. avium* DHFR was the 2′-(5-carboxy-1-butynyl)dibenz[*b*,*f*]azepinyl derivative **20** (IC_{50} = 2.9 nM), whereas the most selective was the 2′-(5-carboxy-1-pentynyl) analogue **21**, with SI values of >100 against both *P. carinii* and *M. avium* DHFR relative to rat DHFR. The final compound, 2,4-diamino-5-[3′-(4-carboxy-1-butynyl)-4′-bromo-5′-methoxybenzyl]pyrimidine (**22**), was both potent and selective against *M. avium* DHFR (IC_{50} = 0.47 nM, SI = 1300) but was not potent or selective against either *P. carinii* or *T. gondii* DHFR.

Introduction

As part of a larger program aimed at the discovery of dihydrofolate reductase (DHFR) inhibitors as potential drugs against the AIDS-associated opportunistic pathogens *Pneumocystis carinii,*[1] *Toxoplasma gondii,* and *Mycobacterium avium*, we have previously studied a small number of 2,4-diamino-5-[2′-methoxy-5′-(ω-carboxyalkoxy)benzyl]pyrimidines (**1**)[2] and 2,4-diamino-5-[(2′-methoxy-ω-carboxy-1-alkynyl)benzyl]pyrimidines (**2**).[3] More recently, we also synthesized and tested the 3′,4′-dimethoxy-5′-(4-carboxy-1-pentynyl) analogue **3**,[4] in which the 3′,4′,5′-trisubstituted pattern of trimethoprim (TMP) is retained. The left half of the molecule in these compounds resembles TMP (**4**) while the right half embodies the 2′,5′-disubstituted pattern of piritrexim (**5**, PTX).

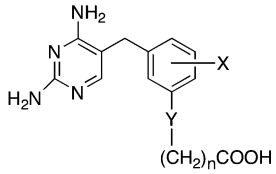

	X	Y	n
1	2′-OMe	OCH_2	2-4
2	2′-OMe	C≡C	2-4
3	3′,4′-$(OMe)_2$	C≡C	3

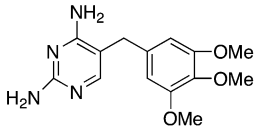

4 (TMP)

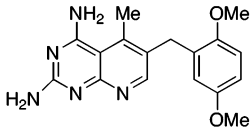

5 (PTX)

While TMP has excellent species selectivity in its binding to nonmammalian vs mammalian DHFR, its potency as a DHFR inhibitor is relatively low. For this reason, it is clinically useful only when given in combination with a sulfa drug like sulfamethoxazole or dapsone to block de novo reduced folate synthesis.[5] However, a shortcoming of TMP/sulfa drug regimens is that many patients develop allergic reactions to the sulfa drug that can be severe enough to require discontinuation of treatment.[6] The binding of PTX to DHFR is orders of magnitude tighter than that of TMP, but unfortunately this increased potency is achieved at the cost of a dramatic loss of species selectivity. Thus, when PTX is administered to a patient it has to be combined with leucovorin (5-formyltetrahydrofolate) to prevent life-threatening myelosuppression.[7] With these consid-

* To whom correspondence should be addressed. Tel: (617)-632-3117. Fax: 617-632-2410. E-mail: andre_rosowsky@dfci.harvard.edu.
† Dana-Farber Cancer Institute, Harvard Medical School.
‡ Department of Pharmacology and Toxicology, Indiana University.

10.1021/jm0581718 CCC: $30.25
Published on Web 06/07/2005

erations in mind, a goal of our laboratory for several years has been to design DHFR inhibitors that combine the potency of PTX with the species selectivity of TMP. A potentially attractive feature of such compounds is that they might not require coadministration of either a sulfa drug or leucovorin. Encouraged by the finding that several examples of general structures **1** and **2**, seemed to have this desired property,[2,3] we asked ourselves whether similar modification of either the 2′- or 5′-methoxy group in PTX would likewise yield DHFR inhibitors retaining, or exceeding, both the potency of PTX and the species selectivity of TMP. In the present paper, we report the synthesis and DHFR-inhibitory activity of the heretofore unknown PTX analogues **6**−**14**. A novel feature of these compounds that sets them sharply apart from PTX is the presence of an ionizable COOH, which confers solubility in water at physiological pH without the need to formulate the drug as a salt.

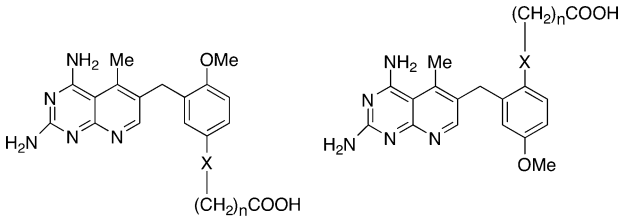

	X	n
6-8	OCH_2	2-4
10-12	C≡C	2-4

	X	n
9	OCH_2	2
13,14	C≡C	2,3

In other work on compounds with a one-carbon bridge between the heterocyclic moiety and the substituted phenyl ring of the side chain, we recently also described the novel pteridines **15**−**18**, of which two, **16** ($n = 1$) and **17** ($n = 2$), displayed the level of potency (IC_{50} < 10 nM) and selectivity (>100-fold against the DHFR from at least two of the three nonmammalian species) that we sought to achieve.[8] Thus, in addition to the pyridopyrimidines **6**−**14**, we synthesized the pteridines **19**−**21** as analogues of **16**−**18** with a carbon−carbon triple bond in place of the OCH_2 group in the side chain. As with **10**−**14**, a potentially useful feature of **19**−**21** is aqueous solubility at physiologic pH. Last, as an extension of our work on the TMP analogue **3**, we synthesized 2,4-diamino-5-[3′-methoxy-4′-bromo-5′-(4-carboxy-1-butyl)benzyl]pyrimidine (**22**). Interest in this previously unknown compound was prompted by a desire to ascertain how removal of the putative out-of-plane hydrophobic interaction of the 4′-methoxy group in **3** might influence selectivity against *P. carinii*, *T. gondii*, and *M. avium* DHFR vs rat DHFR. Compound **22** may be viewed as an analogue of brodimoprim (**23**), which was initially reported to have some advantages over TMP but was subsequently withdrawn from the market.[9,10]

Chemistry

A reasonable approach to the synthesis of the 2′-methoxy-5′-(ω-carboxyalkoxy) analogues **6**−**8** seemed to be via the sodium salt **24**, which was accessible in three steps from 4-hydroxyanisole by sequential reaction with methyl chloroformate, Lewis acid-catalyzed condensation with dichloromethoxymethane, and finally treat-

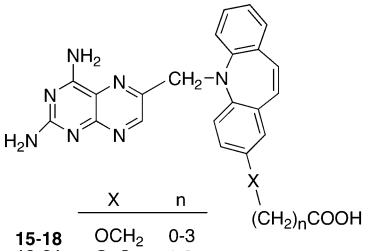

	X	n
15-18	OCH_2	0-3
19-21	C≡C	1-3

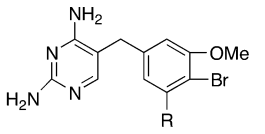

22: R = C≡C(CH2)2COOH
23: R = OMe (brodimoprim)

ment with NaOMe.[2] As shown in Scheme 1, *O*-alkylation of rigorously dried **24** with benzyl bromide afforded the known compound **25**, which on Knoevenagel condensation with ethyl acetoacetate followed by catalytic hydrogenation was converted to the β-ketoester **26**. Then, in an adaptation of the method originally developed for the synthesis of PTX by Grivsky and coworkers,[11a] and later improved by Rauckman and coworkers,[11b] **26** was heated with 2,4,6-triaminopyrimidine in *N*-methyl-2-pyrrolidinone (NMP), and the resulting lactam **27** was converted to **28** with oxalyl chloride in DMF. Debenzylation and dechlorination of **28** were then achieved in a single step with 5% Pd−C and sodium formate in 2-methoxyethanol.[12] To complete the synthesis, the thoroughly dry Na salt of the resulting phenol **29** was treated overnight at room temperature with ethyl 4-bromobutanoate, 5-bromopentanoate, or 6-bromohexanoate in dimethylsulfoxide (DMSO) solution to obtain, after purification by chromatography and recrystallization, the esters **30**−**32**. Saponification then yielded the desired acids **6**−**8**. Although the heterocyclic intermediates **27**−**29** were used without extensive purification, the structure and purity of each of the esters **30**−**32** and acids **6**−**8** was established from ^1H NMR and mass spectra and by microchemical analysis.

For the preparation of the 2′-modified analogue **9**, we initially tried to adopt with minor modifications an approach developed by Troschütz and co-workers[13] for the synthesis of PTX. Thus, as shown in the upper half of Scheme 2, the Wittig reaction between 2-benzyloxy-5-methoxybenzaldehyde (**33**) and 1-triphenylphosphoranylidene-2-propan-one followed by catalytic hydrogenation afforded the ketone **34**, which on Vilsmeier reaction ($POCl_3$/DMF) afforded the expected mixture **35a/35b**. The geometrical isomers migrated with different R_f values on thin-layer chromatography (TLC) and were separated by flash chromatography. The two isomers could be distinguished easily by ^1H NMR, with the aliphatic Me group of the minor *Z*-isomer (18% isolated yield) giving a singlet at δ 2.25 whereas the corresponding peak for the major *E*-isomer (41% isolated yield) was shifted downfield to δ 2.68. Condensation of the *E*/*Z* mixture with cyanoacetamide proved more difficult than initially anticipated, as the isolation of the desired product **36** required extensive column chromatography with monitoring of individual fractions by ^1H NMR. After considerable effort, pure **36** was obtained in 45% yield and was converted first to the chloronitrile **37** with oxalyl chloride and then to the key intermediate **38** with guanidine free base in refluxing pyridine.

While we had intended originally to remove the *O*-benzyl group at this stage and then the *O*-alkylate, resulting in a product with a bromo ester as in the synthesis of **30**−**32**, the ^1H NMR spectra of the unpurified product of the cyanoacetamide reaction of **35a/**

Scheme 1[a]

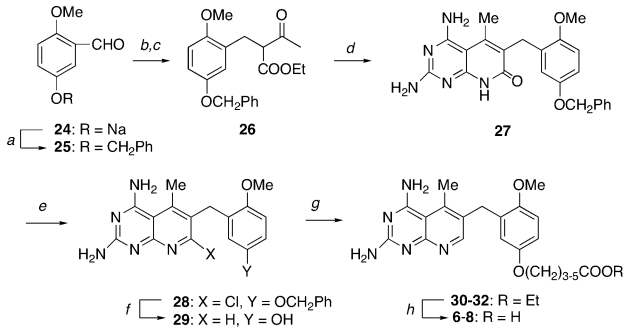

[a] Reagents and conditions: (a) $PhCH_2Br$, DMF; (b) $MeCOCH_2COOEt$, toluene, AcOH, piperidine, reflux; (c) H_2/5% Pd−C; (d) 2,4,6-triaminopyrimidine, NMP, 190 °C; (e) $(COCl)_2$, DMF; (f) HCOONa, 5% Pd−C, $MeOCH_2CH_2OH$, reflux; (g) NaOEt, DMSO, then $Br(CH_2)_{3-5}COOEt$; (h) NaOH, EtOH.

35b indicated that it probably contained in addition to lactam **36** a certain amount of its sterically less crowded 6-methyl isomer **36a** whose complete removal was exceedingly laborious. Thus, we abandoned further use of **36** as an intermediate and turned instead to the original approach using a β-ketoester rather than a β-chlorovinyl ketone. As shown in the lower half of Scheme 2, aldehyde **33** was reduced to alcohol **39** with $NaBH_4$, **39** was converted to the chloride **40** with thionyl chloride, and **40** was condensed with the Na salt of ethyl acetoacetate in refluxing THF to form the substituted β-ketoester **41**. Further elaboration of **41** via intermediates **42**−**45** then led to the acid **9**.[14]

The method used to obtain **9** could presumably be extended to other 2′-(ω-carboxyalkoxy)-5′-methoxy homologues. However, the interesting results we had obtained earlier with the acetylenic diaminopyrimidine derivatives **2** prompted us to focus instead on ω-carboxy-1-alkynyl analogues of PTX. As shown in Scheme 3, these compounds were prepared via the intermediates **47**−**54**, which were obtained from 2- and 3-methoxybenzaldehyde, respectively, via the classical β-ketoester route (cf. Scheme 2). Treatment of **53** and **54** with *N*-iodosuccinimide in TFA yielded the iodides **55** and **56**, respectively, and the latter were condensed with benzyl ω-alkynoates in the presence of $(Ph_3P)_2PdCl_2$, CuI, and Et_3N in a Sonogashira reaction.[17] The resulting esters **57**−**61** were then saponified to the acids **10**−**14** to complete the synthesis.

Since it was important to be sure that the products ultimately used in DHFR assays had the correct pattern of substitution on the phenyl ring, the position of the iodine atom in **55** and **56** was confirmed by ^{1}H NMR. The 3′-proton in the phenyl ring was found to give a doublet at δ 6.8 in **55** and δ 7.8 in **56**, the 4′-proton a doublet of doublets at δ 7.5 in **55** and δ 6.6 in **56**, and the 6′-proton a doublet at δ 7.1 in **55** and δ 6.4 in **56**. Moreover, the coupling constants for each aromatic proton were consistent with the assigned 1,2,5-trisubstituted structures, thereby excluding any possibility that iodination had occurred next to the methoxy group.

For the synthesis of the third group of compounds described in this paper, the dibenz[*b*,*f*]azepine derivatives **19**−**21**, we took advantage of the ability of alkynes to react with aromatic triflate esters in the presence of a Pd(0) catalyst. Thus, as shown in Scheme 4, treatment of *N*-(2,4-diaminopteridin-6-yl)methyldibenz[*b*,*f*]azepin-2-ol (**62**)[8] with triflic anhydride in pyridine at ambient temperature for 3 h, followed by flash chromatography on silica gel, afforded a product whose ^{1}H NMR spectrum confirmed it to be the desired triflate **63**. Overnight treatment of purified **63** at 90 °C with benzyl 3-butynoate, benzyl 4-pentynoate, or benzyl 5-hexynoate in the presence of $(Ph_3P)_2PdCl_2$ and Et_3N yielded the esters **64**−**66**, which were saponified directly with NaOH to obtain the acids **19**−**21**. For purification, the latter were subjected to a two-stage sequence consisting of anion exchange chromatography on a Dowex 50W-X2-100 resin followed by adsorption chromatography on deactivated silica gel.

Initial attempts to prepare the bromide **22** were made directly from the *O*-triflate ester of the known compound 2,4-diamino-5-(3′-hydroxy-4′-bromo-5′-methoxybenzyl)-pyri-midine (**67**).[18] However, a few test reactions of **67** with trifluoromethylsulfonyl chloride or triflic anhydride in pyridine were found to give complicated mixtures of *O*- and *N*-trifluoromethylsulfonyl derivatives, presumably indicating the more reactive nature of the NH_2 groups in **67** than those in **62**. In addition, we were concerned that an acidic NHTf group on the heterocyclic moiety could create a problem during the alkynylation step by coordinating with the Pd catalyst. While they are not commonly used for N-protection in diaminopyrimidines, we were pleased to find that Boc groups served our purpose quite well. Thus, as shown in Scheme 5, treatment of **67** with excess Boc anhydride in the presence of Et_3N and DMAP afforded a 67% yield of a noncrystalline product whose ^{1}H NMR spectrum was consistent with the fully Boc-substituted structure **68**. Selective cleavage of the *O*-Boc group in **68** with morpholine in CH_2Cl_2 (1:3, v/v) at room temperature then yielded the desired phenol **69** (53% yield) along with two slightly more polar byproducts that were separable from **69** by chromatography and whose ^{1}H NMR spectra showed only three *N*-Boc groups, indicating that partial N-deprotection had also taken place. To complete the synthesis **69** was converted to the fully N-protected triflate ester **70** (95% yield) with triflic anhydride in pyridine, and **70** was warmed with benzyl 4-pentynoate in the presence of $(Ph_3P)_2PdCl_2$, $(Ph_3P)_3$-CuBr, and Et_3N at 55 °C for 3 h to obtain ester **71**, from which the Boc groups and the benzyl ester group were all removed at the same time by a reaction with NaOH in DMSO. The final product **22** was purified by preparative high-performance liquid chromatography (HPLC) on C_{18} silica gel followed by ion-exchange chromatography on (diethylamino)ethyl (DEAE)-cellulose. The two-step yield of **22** from **71** was 20%.

Enzyme Inhibition Assays. The ability of acids **6**−**14** and **19**−**22** to inhibit dihydrofolate reduction by *Pneumocystis carinii*, *Toxoplasma gondii*, *Mycobacterium avium*, and rat DFHR in the presence of NADPH was determined spectrophotometrically at 340 nm as previously described.[19] The *P. carinii* DHFR used in these assays was recombinant enzyme cloned from organisms isolated from the lungs of infected rats.[19] Also tested were the esters **30**−**32**, the benzyl ether **38**, and the iodides **55** and **56** as additional examples of PTX analogues in which one or the other methoxy group is replaced. The IC_{50} values, selectivity index (SI), and 95% confidence limits of all of the compounds are shown in

Scheme 2[a]

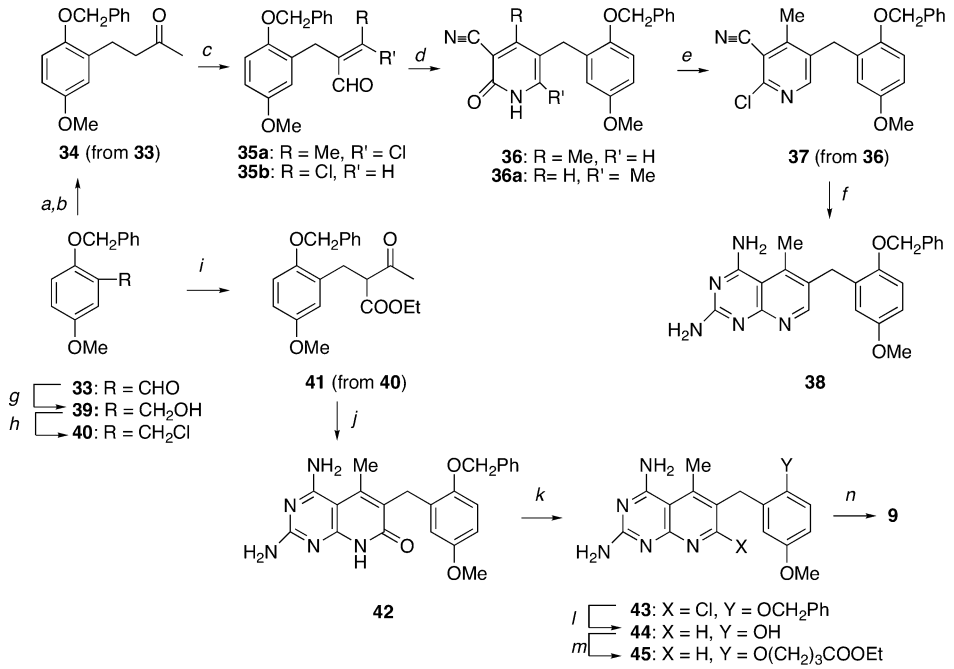

[a] Reagents and conditions: (a) $Ph_3P{=}CHCOMe$; (b) H_2, PtO_2; (c) $POCl_3$, DMF; (d) $N{\equiv}CCH_2CONH_2$, NaH, THF, reflux; (e) $(COCl)_2$, DMF, 0 °C; (f) guanidine, pyridine, reflux; (g) $NaBH_4$, MeOH; (h) $SOCl_2$, benzene; (i) $MeCOCH_2COOEt$, NaH,THF, reflux; (j) 2,4,6-triaminopyrimidine, NMP, 190 °C; (k) $(COCl)_2$, DMF, 0 °C; (l) HCOONa, 5% Pd−C, $MeOCH_2CH_2OH$, reflux; (m) NaOEt, DMSO, then $Br(CH_2)_3COOEt$; (n) NaOH, EtOH.

Scheme 3[a]

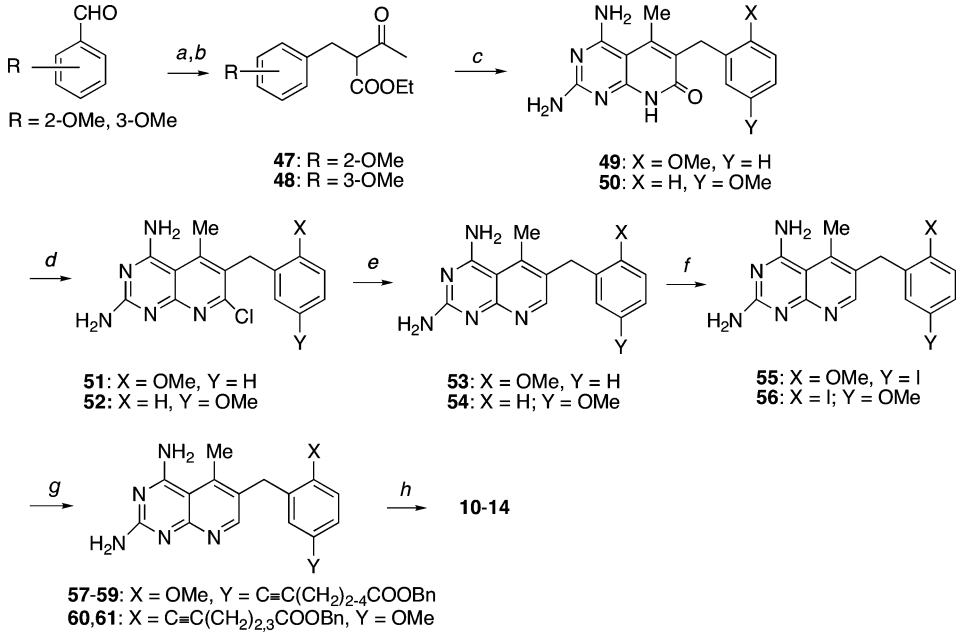

[a] Reagents and conditions: (a) $MeCOCH_2COOEt$, piperidine, AcOH, toluene, reflux; (b) H_2/5% Pd−C; (c) 2,4,6-triaminopyrimidine, NMP, 190 °C; (d) $(COCl)_2$, DMF, CH_2Cl_2; (e) HCOONa, 5% Pd−C, $MeOCH_2CH_2OH$, reflux; (f) *N*-iodosuccinimide, TFA; (g) $HC{\equiv}C(CH_2)_nCOOBn$ (n = 2−4),$(Ph_3P)_2PdCl_2$, CuI, Et_3N; (h) NaOH, EtOH.

Table 1. Also presented for comparison are data we have already reported for TMP (a weak but selective inhibitor), PTX (a potent but nonselective inhibitor), and compound **3**, an example of a DHFR inhibitor which is both potent and selective.

(a) *Pneumocystis carinii* DHFR. The 2′-methoxy-5′-(ω-carboxyalkyl)oxy analogues **6**−**8** were all potent inhibitors of recombinant DHFR from rat *P. carinii*,[20] with IC_{50} values of approximately 0.1−1.0 nM as compared with 13 nM for PTX. Moreover, while PTX was completely nonselective for *P. carinii* vs rat DHFR (SI = 0.26), these compounds all displayed a small degree of selectivity, and of these, the *O*-(carboxypropyl) analogue **6** was 30 times more potent than PTX and was mildly selective (SI = 5.1). Interchanging the positions of the *O*-methyl and *O*-(carboxypropyl) groups as in **9** led to a 2.5-fold increase in binding and a higher degree of selectivity (SI = 54) than that found in **6**. Thus, it appeared that binding was more favorable when the *O*-carboxyalkyl side chain projected into the active site

Scheme 4[a]

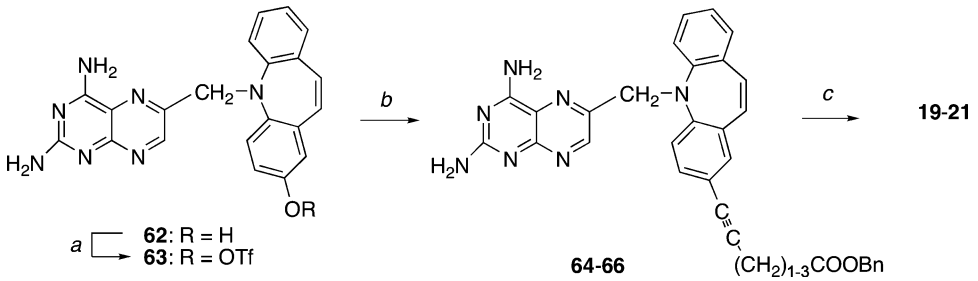

[a] Reagents and conditions: (a) Tf_2O, pyridine, rt, 3 h; (b) HC≡C$(CH_2)_{1-3}$COOBn, $(Ph_3P)_2PdCl_2$, Et_3N, DMF; (c) NaOH.

Scheme 5[a]

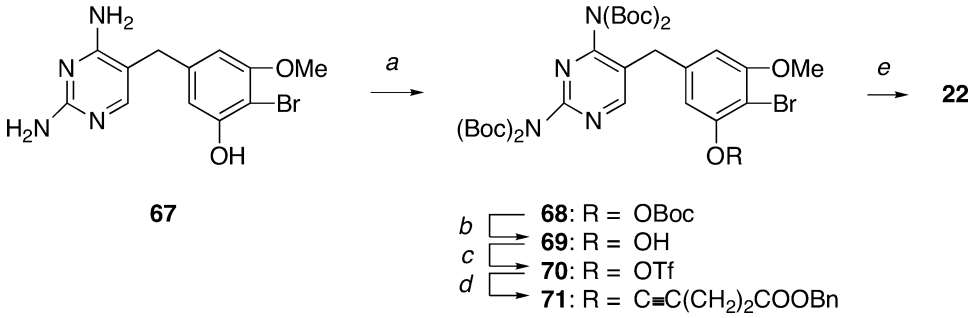

[a] Reagents and conditions: (a) Boc_2O, Et_3N, DMAP, rt, 20 h; (b) 25% morpholine/CH_2Cl_2 (25% v/v), rt, 3 h; (c) Tf_2O, pyridine, 0 °C, 20 h; (d) HC≡C$(CH_2)_2$COOB*n*, $(Ph_3P)_2PdCl_2$, $(PhP)_3CuBr$, Et_3N, DMF, 55 °C, 20 h; (e) NaOH.

from the 2′-position of the benzyl group than from the 5′-position.

Replacing the OCH_2 moiety in **6**−**8** by a carbon−carbon triple bond, which has the effect of straightening and stiffening the side chain, led to improved binding to *P. carinii* DHFR in the case of **10** vs **6**, but not in the case of **11** vs **7** or **12** vs **8**, suggesting that the effectiveness of this molecular modification depends on the overall length of the side chain. Compound **10** was ca. 130-fold more potent than PTX against *P. carinii* DHFR, but because its binding to the rat enzyme was even tighter than that of **9**, there was a 16-fold loss of selectivity (SI = 3.3). In our previous work on analogues of TMP, we had observed that replacement of OCH_2 by C≡C was also somewhat favorable, though only when compounds with a relatively short side chain (i.e., **1** and **2**, $n = 2$) were compared. However, given the much greater potency of PTX vs TMP against *P. carinii* DHFR, we were disappointed to find that our 2′,5′-disubstituted PTX analogues were not more selective than the 2′,5′-disubstituted TMP analogues with similar side chains that we had studied earlier. Turning next to the analogues with ω-carboxy-1-alkynyl groups of approximately the same length at the 2′-position instead of at the 5′-position, **13** was found to be less potent than **10**, whereas in the longer homologues **14** and **11** a difference was no longer evident.

With regard to the esters **30**−**32** and **45**, it was of interest to note that, with the exception of the shortest-chained analogue **30**, a substantial loss of binding occurred vís a vís the corresponding acids, supporting the idea that a COOH group is favorable for binding to the *P. carinii* enzyme regardless of whether it projects into the active site from the 5′- or 2′-position of the benzyl moiety. Not surprisingly, there was only a minor difference in potency and selectivity between the iodides **55** and **56** in comparison with PTX itself. However there was a ca. 7.4-fold decrease in binding between the 2′-*O*-benzyl ether **38** and PTX, and a 25-fold binding between **38** and the 2′-iodide **56**, presumably reflecting the bulky nature of the *O*-benzyl group.

Turning to the dibenz[*b*,*f*]azepine analogues **19**−**21** with ω-carboxy-1-alkyl groups at the 2′-position, the inhibition data against *P. carinii* DHFR in Table 1 revealed a striking degree of dependence on the number of CH_2 groups. Thus, while **19** and **21** had IC_{50} values of 9.4 and 12 nM, respectively, that of **20** (230 nM) was ca. 20-fold higher. Similarly, while **20** showed no selectivity, the SI values of **19** and **21** were in the range of 80−100. This was not entirely surprising, as we had reported earlier a similar, albeit less steep, correlation of the IC_{50} value with the number of side chain CH_2 groups among the *O*-ω-carboxyalkyl analogues **16**−**18**, with **17** (IC_{50} = 1.1 nM, SI = 1300) showing a 1-log improvement in potency relative to the other compounds in the series.

The brodimoprim analogue **22** was a more potent inhibitor than TMP, but was also less selective, reflecting a greater increase in binding to rat DHFR than to *P. carinii* DHFR. It is also worth nothing that **22** was a poorer inhibitor of *P. carinii* DHFR than the corresponding TMP analogue **3** but was a better inhibitor of the rat enzyme. Because the congener of **22** with one additional CH_2 group in the side chain was not available for comparison, it cannot be said at this time whether the difference between **3** and **22** is due to the change of the 4′-substituent from OMe to Br or to the fact that the carboxyalkynyl chain is shorter by one carbon.

Overall, the results in Table 1 indicate that all of the new compounds studied fall well short of the potency and selectivity of **3**, which remains the benchmark among all of the compounds we have tested to date.

(b) *Toxoplasma gondii* DHFR. The 5′-*O*-carboxyalkyl analogues **6**−**8** and the 2′-*O*-carboxyalkoxy ana-

Table 1. Inhibition of Dihydrofolate Reductases by 2,4-Diaminopyrido[2,3-*d*]pyrimidine and 2,4-Diaminopteridine Derivatives

	(IC_{50}, nM)				selectivity index[a]		
compd	*P. carinii*	*T. gondii*	*M. avium*	rat	*P. carinii*	*T. gondii*	*M. avium*
3[c]	1.0 (0.82−1.2)	34 (30−39)	2.4 (2.1−2.7)	5000 (4300−5800)	5000 (3600−7100)	150 (110−190)	2100 (2000−2800)
4[c] (TMP)	13000 (10000−16000)[b]	2800 (2400−3300)	300 (260−350)	180000 (160000−210000)	14 (10−20)	65 (48−87)	610 (460−810)
5[c] (PTX)	13 (9.0−17)	4.3 (4.0−4.6)	0.61 (0.53−0.70)	3.3 (2.9−3.9)	0.26 (0.17−0.42)	0.76 (0.63−0.97)	5.4 (4.1−4.7)
6	0.43 (0.37−0.50)	1.9 (1.8−2.0)	0.26 (0.23−0.30)	2.2 (2.0−2.4)	5.1 (4.0−6.5)	1.2 (1.0−1.3)	8.5 (6.7−10)
7	0.51 (0.35−0.75)	2.3 (2.1−2.4)	0.29 (0.23−0.36)	2.2 (1.9−2.8)	4.2 (2.5−8.0)	0.96 (0.79−1.3)	7.5 (5.3−12)
8	1.3 (0.92−1.8)	2.0 (1.8−2.2)	0.35 (0.30−0.39)	2.0 (1.8−2.2)	1.5 (1.0−2.0)	1.0 (0.82−1.2)	5.9 (4.6−7.3)
9	0.17 (0.12−0.23)	2.3 (2.0−2.7)	0.32 (0.29−0.35)	9.1 (6.7−12.5)	54 (29−100)	4.0 (2.5−6.3)	28 (19−43)
10	0.097 (0.086−0.11)	0.46 (0.42−0.51)	0.057 (0.050−0.065)	0.32 (0.28−0.37)	3.3 (2.6−4.3)	0.70 (0.55−0.88)	5.6 (4.3−7.4)
11	1.4 (1.2−1.5)	4.3 (3.8−4.9)	1.0 0.94−1.1)	5.7 (5.1−6.4)	4.2 (3.4−5.3)	1.3 (1.0−1.7)	5.6 (4.6−6.8)
12	1.8 (1.6−2.0)	3.2 (2.9−3.6)	0.69 (0.63−0.74)	4.0 (3.6−4.5)	2.2 (1.8−2.8)	1.3 (1.0−1.6)	5.8 (4.9−7.1)
13	0.65 (0.58−0.73)	4.1 (3.5−4.8)	0.57 (0.52−0.63)	55 (51−60)	85 (70−100)	13 (11−17)	96 (81−120)
14	1.2 (1.0−1.3)	5.8 (5.0−6.7)	1.3 (1.1−1.4)	24 (19−29)	20 (15−29)	4.1 (3.8−5.8)	18 (14−21)
19	9.4 (7.9−11)	100 (81−130)	17 (13−22)	740 (640−860)	79 (58−110)	7.4 (4.9−11)	43 (29−66)
20	230 (200−260)	77 (71−83)	2.9 (2.4−3.4)	560 (480−650)	2.4 (1.9−3.3)	7.3 (5.8−9.2)	190 (140−270)
21	12 (8.4−17)	21 (19−24)	6.3 (4.8−8.3)	1300 (1100−1500)	110 (65−180)	62 (46−79)	210 (130−310)
22	71 (58−87)	15 (14−16)	0.47 (0.37−0.62)	630 (530−750)	8.9 (6.1−12.9)	42 (39−46)	1300 (850−2100)
30	6.5 (5.7−7.3)	3.4 (3.0−3.8)	1.8 (1.3−2.5)	4.2 (3.6−5.0)	0.65 (0.49−0.68)	1.2 (0.95−1.7)	2.3 (1.4−3.9)
31	28 (24−33)	11 (4.9−6.5)	9.4 (8.4−11)	14 (12−16)	0.50 (0.36−0.67)	1.3 (1.9−3.3)	1.5 (1.1−1.9)
32	35 (25−48)	13 (12−13)	12 (10−13)	21 (18−25)	0.60 (0.38−1.0)	1.6 (1.4−2.1)	1.8 (1.4−2.5)
38	96 (84−110)	16 (9.6−14)	8.6 (7.2−10)	170 (130−220)	1.8 (1.2−2.6)	11 (9.3−23)	20 (13−31)
45	83 (77−90)	10 (7.7−14)	5.6 (4.7−6.6)	93 (87−101)	1.1 (0.97−1.3)	9.1 (6.2−13)	17 (13-21)
55	5.8 (5.0−6.8)	4.1 (3.1−5.4)	0.92 (0.84−1.0)	5.0 (4.2−5.8)	0.86 (0.62−1.2)	1.2 (0.78−1.9)	5.4 (4.2−6.9)
56	3.8 (3.6−4.1)	5.8 (5.6−5.9)	1.8 (1.6−2.0)	4.0 (3.9−4.2)	1.1 (0.95−1.0)	0.69 (0.66−0.75)	2.2 (2.0−2.6)

[a] Selectivity Index (SI) = IC_{50} (rat)/IC_{50} (*P. carinii*, *T. gondii*, or *M. avium*). All of the values are rounded off to two significant figures. [b] Numbers in parentheses are 95% confidence limits. [c] Data for **3**−**5** are taken from refs 1−3.

logue **9** all gave IC_{50} values of ca. 2 nM and were only slightly more potent than PTX, and their selectivity was quite modest. The esters **30**−**32** and **45** showed essentially the same binding activity as the corresponding acids, suggesting that in the case of the binding of these PTX analogues to the *T. gondii* enzyme, a carboxyalkoxy group at either the 5′-position or the 2′-position hardly mattered. The same was also the case generally speaking for the carboxyalkynyl analogues **10**−**14**. It was clear from the results that the addition of a COOH group was much less effective for *T. gondii* DHFR inhibition than for *P. carinii* DHFR inhibition, suggesting that there is little likelihood of an interaction with a basic Lys or Arg residue.

The dibenz[*b*,*f*]azepine analogues **19**−**21** inhibited *T. gondii* DHFR with IC_{50} values in the 20−100 nM range and thus were more potent than TMP but less potent than PTX. Although **21** did have a respectable SI value of 62, neither its potency nor its selectivity equaled that of **17** (IC_{50} = 9.9 nM, SI = 120).[8] As in the case of the *P. carinii* enzyme, the potency and selectivity of **22** exceeded that of TMP but was unremarkable in comparison with **3**. Again, however, it would be of interest to test the congener of **22** with one more carbon in the side chain, but this compound was not made.

(c) *Mycobacterium avium* DHFR. The 5′-*O*-carboxyalkyl analogues **6**−**8** and the 2′-*O*-carboxyalkyl analogue **9** inhibited *M. avium* DHFR with IC_{50} values in the 0.2−0.4 nM range, but **9** (SI = 28) was considerably more selective than the others. The corresponding esters were 5−10 times less potent, suggesting that a COOH group in the side chain of the inhibitor may be able to interact with a basic Arg or Lys residue in the active site of the enzyme, as seems to be the case for the *P. carinii* enzyme. The 5′-(ω-carboxy-1-alkynyl) analogues **10**−**12** and the 2′-(ω-carboxy-1-alkynyl) analogues **13** and **14** inhibited the enzyme with IC_{50} values several times higher than those of the ethers **6**−**9**. However, despite the fact that it was less potent than some of the other acids, the 2′-(4-carboxy-1-butynyl) analogue **13** appeared to be by far the most selective for *M. avium* vs rat DHFR (SI = 96) just as it was for the *P. carinii* enzyme (SI = 85).

Turning to the dibenz[*b*,*f*]azepines as inhibitors of *M. avium* DHFR, the most potent was the 4-carboxy-1-butynyl derivative **20**, with IC_{50} and SI values of 2.9

Table 2. In Vitro Growth Inhibition of CCRF-CEM Leukemic Lymphoblasts by Selected Piritrexim Analogues[a]

compd	IC_{50} (μM)[b]	compd	IC_{50} (μM)[b]
5 (PTX)	0.013 ± 0.0023[c]	**11**	6.1 ± 0.33
6	3.7 ± 1.1	**14**	2.8 ± 0.56
9	5.3 ± 1.1		

[a] Assays were carried out as described previously. [b] Each IC_{50} is the mean ± SD of three separate experiments on different days. [c] Numbers are rounded off to two significant figures.

nM and 190, respectively. However, the activity of the 5-carboxy-1-pentynyl analogue **21** was essentially the same. Activity and potency both decreased when the carboxyalkynyl arm was shortened by one CH_2 group as in **19**. In comparison with the previously reported data for the ethers **15**−**18**,[8] compound **20** once again most closely resembled **17** (IC_{50} = 2.0 nM, SI = 600) in potency but was 3 times less selective. All in all, there was a gratifying degree of qualitative consistency in structure−activity trends against all three of the parasite enzymes between the 2′-(ω-carboxy-1-alkynyl)-dibenz[*b*,*f*]azepines in this paper and the 2′-*O*-(ω-carboxyalkyl) analogues we had studied earlier. However, as noted above, none of the new compounds matched the remarkable potency and selectivity of **3**,[4] indicating that a carboxyalkoxy or carboxyalkynyl arm is more effective on a diaminopyrimidine scaffold than on a diaminopyrido[2,3-*d*]pyrimidine or diaminopteridine scaffold.

The brodimoprim analogue **22** was notable for the fact that it combined high potency (IC_{50} = 0.47 nM) with >1000-fold selectivity. Because its potency against *M. avium* DHFR was several times greater than that of **3**, this compound could represent an exploitable lead (e.g., by substituting other alkoxy groups for OMe at the 3′-position or changing the length of the 5′-carboxyalkynyl chain).

In Vitro Growth Inhibition Assays. Because our therapeutic intent in synthesizing the PTX analogues in this paper was to assess their therapeutic potential in the treatment of AIDS-associated opportunistic infections in humans, we compared the activity of four selected examples (**6**, **9**, **11**, and **14**) as inhibitors of the growth of cultured CCRF-CEM human leukemic lymphoblasts in a 72 h assay routinely used in our laboratory.[21] Since there are no data as of yet on the ability of these compounds to prevent growth of *P. carinii*, *T. gondii*, or *M. avium* parasites in culture, the purpose of this experiment was not to show that the compounds could selectively block the growth of the parasites in the presence of mammalian host cells but merely to ascertain whether they could get into mammalian cells at a concentration likely to be physiologically achievable (<10 μM), as well as determine how their potency as cell growth inhibitors would compare with their activity as DHFR inhibitors and how these would compare with the activity of PTX. As shown in Table 2, the four compounds we tested all had similar IC_{50} values in the 1−10 μM range. Not surprisingly, in light of the presence of a COOH group in the side chain, they were considerably less (>200-fold) potent than PTX despite their much smaller differences in potency relative to PTX in terms of binding to isolated DHFR enzymes (cf. for example, the data against rat DHFR). The IC_{50} value varied over a broader range than the IC_{50} value against intact cells, suggesting that uptake rather than DHFR binding may be the limiting factor in the ability of the analogues to inhibit growth. At this point, it is unknown how these lipophilic, yet negatively charged, molecules are transported into cells. Studies addressing this issue could be of interest in view of the fact that uptake of these compounds across cell membranes may be more complex than simply by partition in and out of the lipid bilayer. Given the nearly 2-log selectivity of **13** at the level of both *P. carinii* and *M. avium* DHFR inhibition, the design of prodrugs of this compound might be worthwhile to consider.

It should be noted that in vivo studies of the compounds in this paper were not done, and we therefore cannot say anything about the metabolic and/or pharmacokinetic differences that may exist between **6**−**14** and PTX on one hand and between **22** and brodimoprim on the other. While such studies could be of interest in the future, they were not considered to be the scope of the present work.

Molecular Modeling

A crystal structure of the ternary complex of PTX and TMP with NADPH and *P. carinii* DHFR had already been reported by Champness and co-workers[22,23] when this work began, but unfortunately the three-dimensional (3D) coordinates of the ternary complex with PTX were not in the public domain. PTX and TMP, according to the published information, bind similarly to the active site, the most notable difference being a conformational change of the Phe69 side chain in the case of the PTX complex, resulting in a face−edge interaction with the dimethoxybenzyl group that was absent in the case of the TMP complex. Interestingly, the 2′-OMe group of PTX occupied a position close to the 3′-OMe group of TMP. Unlike the trimethoxybenzyl group in TMP, the dimethoxybenzyl group in PTX did not make van der Waals contact with the nicotinamide group of NADPH. There were 15 pairwise van der Waals contacts with active site residues for TMP as compared with 20 for PTX. The larger pyridopyrimidine moiety positions the benzyl side chain nearer to the region encompassing residues 65−69 than was the case with TMP. However neither inhibitor had a side chain that was long enough to reach the conserved Arg75 residue, a site with which classical antifolates such as MTX can interact strongly via the α-COOH group of the glutamate moiety. In the crystal structure of the TMP ternary complex, electron density was observed in this otherwise empty pocket, and the density was believed to arise from two bound water molecules.

There are two critical differences between the *P. carinii* and human DHFR active sites; Lys37 and Phe69 in the *P. carinii* enzyme are replaced by Gln35 and Asn64, respectively, in the human enzyme. In the case of our recently described 2′-O-(ω-carboxyalkyl)]dibenz-[*b*,*f*]azepine derivatives **15**−**18**, improved binding selectivity for the *P. carinii* enzyme was attributed to a combination of hydrogen bonding to Lys37 and van der Waals interaction with Phe69.[8] Furthermore, previous structure determinations indicated that Asn64 in human DHFR interacts with the COOH group of MTX.[24] Guided by this background information, we performed manual docking studies with two of the compounds

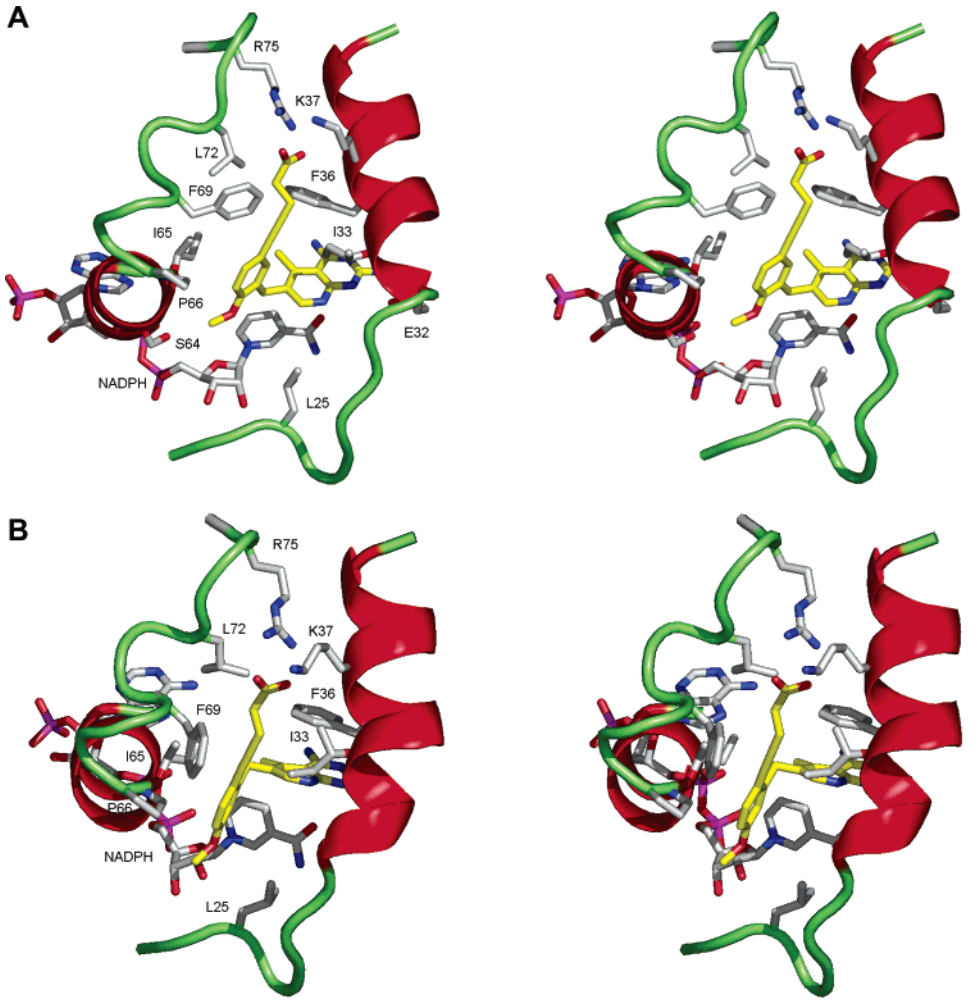

Figure 1. Stereoview of the active site ternary complexes of **10** (panel A) and **13** (panel B) with *Pneumocystis carinii* DHFR and NADPH after an unrestrained 1-ns molecular dynamics simulation using the program AMBER-7[26] as described.[8] Model generated using the PYMOL molecular graphics system.

synthesized in the present work, namely, the acids **10** and **13**, in which the alkyne side chain is more linear and rigid than it would be in an ether side chain. Molecular dynamic simulations were performed as described in a previous paper, and a pictorial representation is given in Figure 1.

Notable interactions in **10** appeared to include H bonds of the COOH group to the distal nitrogens of Arg75 (3.3 and 2.9 Å) or the ϵ-amino group of Lys37 (3.1 Å). There also appeared to be a conformational change in the Phe69 side chain that allowed the formation of a number of van der Waals contacts (3.7−4.0 Å) with the alkynyl chain. In addition, Ile65 interacted extensively with the benzyl moiety and Ile33 interacted with the A ring of the heterocyclic moiety (ca. 4 Å). As in the case of the TMP ternary complex, the CH_2 bridge made van der Waals contacts with the nicotinamide moiety of NADPH.

For compound **13**, the orientation of the benzyl ring was similar to that of PTX.[22] The COOH group appeared to be able, once again, to form H bonds with the distal nitrogens of Arg75 (3.1 and 3.0 Å) or the ϵ-amino group of Lys37. In addition, there was van der Waals contact between the alkynyl side chain and Leu72 (4.3 Å), Ile33 (4.1 Å), and the phenyl ring of Ph69 (3.6−3.8 Å). Unlike the 2′-OMe group in **10**, which H bonds to the OH group of Ser64, the 5′-OMe group in **13** was located 3.9 Å from the carbonyl backbone of this residue and does not interact with the OH. As in the complex of **10**, The CH_2 bridge of **13** again came within the van der Waals distance of the nicotinamide group of NADPH (4.1 Å), but rather distinctively, the CH_2 bridge was tilted 2.2 Å further into the active site, allowing the carboxyalkynyl arm of the inhibitor to project into the region of Arg75 and Lys37 despite being on the 2′- as opposed to the 5′-carbon of the phenyl ring. All in all, the degree of similarity of the interaction of **10** and **13** with the enzyme was quite striking and was consistent with the absence of a dramatic difference in binding as measured by spectrophotometric assay.

The outcome of the dynamics simulations suggested that both Arg75 and Lys37 could interact with the bound ligands (Figure 1), and their moderate SI value seemed to reinforce the hypothesis that, while the presence of Lys37 in the *P. carinii* enzyme as opposed to Gln35 in the human enzyme might confer selectivity in the case of TMP analogues despite the fact that Arg75 is conserved, the effect of the latter takes precedence where PTX analogues are concerned. A summary of the individual active residues that contributed to the simulated binding of **10** and **13** to *P. carinii* DHFR is given in Table 3 of Supporting Information. When the inter- and intramolecular interactions of the inhibitors with all of the residues in the active site were summed up,

the calculated energy of interaction for **10** (−214.48 kcal/mol) proved slightly lower than that of **13** (−196.87 kcal/mol), in qualitative agreement with the finding that the former was slightly more potent. The simulation clearly suggests that, with some relatively minor spatial realignments of a few key amino acid residues and a small change in the relative conformation of the two halves of the ligand, binding is possible for either 2′- or 5′-modified series of the PTX analogues. On the basis of these results, a reasonable approach to the design of better inhibitors of rat *P. carinii* DHFR based on the PTX scaffold might be to modify the side chain of **10** in such a way that the COOH group could project further toward Lys37 while further improving van der Waals contacts to Phe69. However, it must be stressed that the modeling studies described here were done only for the interaction of **10** and **13** with DHFR from rat *P. carinii* and would be of limited value in predicting the interactions of these compounds, or analogues thereof, with the human pneumocystis strain *P. jirovecii*, in which both the basic Lys37 residue and the Phe69 residue are replaced by serine.[25] Selective inhibitors of *P. jirovecii* vs human DHFR would obviously be more important clinically than selective inhibitors of *P. carinii* vs rat DHFR. At present, our ability to address this problem via rational structure-based drug design is limited by the lack of published 3D structures for *P. jirovecii* DHFR ternary complexes with NADPH and lipophilic antifolates. Once the structural coordinates for at least one *P. jirovecii* ternary complex become available, rapid progress will be likely.

Experimental Section

Melting points were determined on an electrothermal apparatus and are uncorrected. Infrared (IR) spectra (cf. Supporting Information) were measured using KBr disks or thin films pressed between NaCl plates on a Perkin-Elmer double-beam recording spectrophotometer. Only wavelengths above 1200 cm^{-1} are reported. ^1H NMR spectra were recorded at 200 MHz on a Varian instrument. Each resonance is denoted as a singlet (s), doublet (d), doublet of doublets (dd), triplet (t), quartet (q), or multiplet (m). Low-resolution mass spectra (MS) were provided by the Molecular Biology Core Facility of the Dana-Farber Cancer Institute. Precoated Whatman MK6F silica gel plates were used for TLC and were visualized under UV light. Flash column chromatography was performed using "Flash" grade silica gel (Baker, 20 μm particle size). Starting materials and reagents were purchased from Sigma-Aldrich, Fisher Scientific, or Alfa Aesar and were used without further purification unless otherwise stated. Pooled eluates from flash silica gel columns were typically dried over anhydrous Na_2SO_4 prior to rotary evaporation. Elemental analyses were performed by the Robertson Microlit Laboratories, Madison, NJ, and were within ±0.4% of theoretical values except for the found hydrogen values for **10**, **13**, **19**, and **20**, which were uniformly on the low side of this range.

2,4-Diamino-5-methyl-6-[2′-methoxy-5′-(3-carboxypropyl)oxybenzyl]pyrido[2,3-*d*]pyrimidine (6). Ester **30** (60 mg, 0.14 mmol) was dissolved in EtOH (5 mL) with gentle warming, and 2 M NaOH (2 mL) was added; when saponification was complete, as indicated by disappearance of the starting material according to TLC, the yellow solution was adjusted to pH 5 with 10% AcOH, and the precipitate was collected by centrifugation. The pellet was resuspended in a small volume of distilled H_2O and spun down, and the process was repeated two more times. The final pellet was dried in a lyophilization chamber, giving **6** as a white solid (50 mg, 83%): mp 272−273 °C; MS calcd *m/e* 398.18 (MH^+), found 398.27. Anal. ($C_{20}H_{23}N_5O_4 \cdot 0.9AcOH \cdot H_2O$) C, H, N.

2,4-Diamino-5-methyl-6-[2′-methoxy-5′-(4-carboxybutyl)oxybenzyl]pyrido[2,3-*d*]-pyrimidine (7). This compound was obtained in 88% yield from **31** by the same procedure as acid **6**: mp 265−267 °C; MS calcd *m/e* 412.20 (MH^+), found 412.28. Anal. ($C_{21}H_{25}N_5O_4 \cdot 1AcOH \cdot 0.5H_2O$) C, H, N.

2,4-Diamino-5-methyl-6-[2′-methoxy-5′-(5-carboxypentyl)oxybenzyl]pyrido[2,3-*d*]pyrimidine (8). This compound was obtained in 87% yield from **32** by the same method as acid **6**: mp 267−268 °C; MS calcd *m/e* 426.21 (MH^+), found 426.33. Anal. ($C_{22}H_{27}N_5O_4 \cdot 0.6AcOH \cdot 0.4H_2O$) C, H, N.

2,4-Diamino-5-methyl-6-[2′-(3-carboxypropyloxy)-5′-methoxybenzyl]pyrido[2,3-*d*]pyrimidine (9). This compound was prepared from **45** in 80% yield by the same method as acid **6**: mp 268−270 °C; MS calcd *m/e* 398.18 (MH^+), found 398.06. Anal. ($C_{20}H_{23}N_5O_4 \cdot 1.1H_2O$) C, H, N.

2,4-Diamino-5-methyl-6-[2′-methoxy-5′-(4-carboxy-1-butynyl)benzyl]pyrido[2,3-*d*]pyrimidine (10). Iodide **55** (1.3 g, 3.1 mmol) was added to a mixture of benzyl 4-pentynoate (875 g, 4.65 mmol), $(Ph_3P)_2PdCl_2$ (20 mg), CuBr (2 mg), Ph_3P (5 mg), and Et_3N (5 mL) in dry DMF (80 mL). The suspension was kept at 80 °C for 2 days, after which point additional portions of benzyl 4-pentynoate (850 mg), $(Ph_3P)_2PdCl_2$ (10 mg), and CuBr (1 mg) were added and the orange-colored reaction mixture was kept at 80 °C for 3 more days. The solvent was removed by rotary evaporation, and the residue was purified by silica gel flash chromatography (9:1 $CHCl_3$/MeOH, R_f value of 0.26) to obtain ester **57** (0.32 g, 22%). The ester was dissolved directly in EtOH (45 mL) and saponified with 1 M NaOH (5 mL). The EtOH was removed on the rotary evaporator, the residue was taken in H_2O (50 mL), the solution was adjusted to pH 5 with 20% AcOH, and after overnight storage at 4 °C the precipitated solid was collected by centrifugation, washed with cold H_2O, and dried in a lyophilization chamber to obtain **10** as a beige solid (48 mg, 40%): mp >195 °C (dec), gradually turning black above 195 °C; MS calcd *m/e* 392.17 (MH^+), found 392.21. Anal. ($C_{21}H_{21}N_5O_3 \cdot 0.5AcOH \cdot 1.5H_2O$) C, N. H: calcd, 5.87; found, 5.37.

2,4-Diamino-5-methyl-6-[2′-methoxy-5′-(5-carboxy-1-pentynyl)benzyl]pyrido[2,3-*d*]pyrimidine (11). This compound was obtained from iodide **55** and benzyl 5-hexynoate by the same method as **10**: beige solid, mp 255−257 °C, gradually turning black above 195 °C; MS calcd *m/e* 406.19 (MH^+), found 406.06. Anal. ($C_{22}H_{23}N_5O_3 \cdot AcOH \cdot 0.05H_2O$) C, H, N.

2,4-Diamino-5-methyl-6-[2′-methoxy-5′-(6-carboxy-1-hexynyl)benzyl]pyrido[2,3-*d*]pyrimidine (12). This compound was obtained from iodide **55** and benzyl 6-heptynoate by the same method as **10**: beige solid, mp 173−175 °C (dec) turning to a black oil at 192−194 °C; MS calcd *m/e* 420.20 (MH^+), found 420.04. Anal. ($C_{23}H_{25}N_5O_3 \cdot 1.75AcOH \cdot 0.1H_2O$) C, H, N.

2,4-Diamino-5-methyl-6-[2′-(4-carboxy-1-butynyl)-5′-methoxybenzyl]pyrido[2,3-*d*]pyrimidine (13). This compound was obtained from iodide **56** and benzyl 4-pentynoate by the same method as **10**: beige solid, mp 205−207 °C (dec), becoming a black oil at 260−264 °C; MS calcd *m/e* 392.17 (MH^+), found 392.14. Anal. ($C_{21}H_{21}N_5O_3 \cdot 1.2AcOH \cdot 0.8H_2O$) C, N. H: calcd, 5.79; found, 5.10.

2,4-Diamino-5-methyl-6-[2′-(4-carboxy-1-pentynyl)-5′-methoxybenzyl]pyrido[2,3-*d*]pyrimidine (14). This compound was obtained from iodide **56** and benzyl 5-hexynoate by the same method as **10**: beige solid, mp 182−184 °C (dec), becoming a black oil at 198−200 °C; MS calcd *m/e* 406.19 (MH^+), found 406.22. Anal. ($C_{22}H_{23}N_5O_3 \cdot 0.45AcOH \cdot H_2O$) C, H, N.

2,4-Diamino-6-[2′-(3-carboxy-1-propynyl)-5*H*-dibenz[*b*,*f*]azepinyl]methylpteridine (19). Step 1. Triflic anhydride (314 mg, 1.1 mmol) was added an ice-cold solution of **62** (383 mg, 1.0 mmol) in anhydrous pyridine (10 mL), and the mixture was stirred at ambient temperature for 3 h. The solvent was evaporated under reduced pressure, and the residue was treated with 5% $NaHCO_3$, causing a brownish-yellow solid to form. The solid was collected, washed with H_2O,

dried in vacuo, and purified by silica gel flash chromatography (95:5 $CHCl_3$/MeOH) to obtain the triflate ester **63** as a yellow solid (216 mg, 42%) which was sufficiently pure to be used directly in the next step, mp 197 °C.

Step 2. A mixture of freshly prepared **63** (260 mg, 0.50 mmol), benzyl 3-butynoate (87 mg, 0.50 mmol), $(Ph_3P)_2PdCl_2$ (17 mg), and Et_3N (0.75 mL) in dry DMF (40 mL) was stirred at 90 °C overnight under argon. The solvent was removed under reduced pressure, and the residue, consisting of the benzyl ester **64**, was treated with 2 N NaOH (1 mL) followed immediately by the addition of H_2O (60 mL). A small amount of undissolved material was removed by suction filtration, and the clear brownish-yellow filtrate was applied onto a column of Dowex 50W-X2 resin (H^+ form, 2 cm × 20 cm). The column was eluted with H_2O until the eluate was neutral and UV transparent, after which the product was eluted with 1.5% NH_4OH. Appropriately pooled fractions of the eluate were reduced to a small volume by rotary evaporation, followed by freeze drying for 72 h. The residue was purified further by silica gel chromatography using 85:15:5 $CHCl_3$/MeOH/concentrated NH_4OH as the eluent. Appropriate fractions were combined and evaporated under reduced pressure to obtain the hydrated partial ammonium salt of **19** as a dark yellowish-brown solid (32 mg, 14%): mp 218 °C (dec) with preliminary darkening; MS calcd *m/e* 449.16 (MH^+), found 449.06. Anal. ($C_{25}H_{19}N_7O_2 \cdot 0.8NH_3 \cdot 4.5H_2O$) C, N. H: calcd, 5.64; found, 4.86.

2,4-Diamino-6-[2′-(4-carboxy-1-butynyl)-5*H*-dibenz[*b*,*f*]-azepinyl]methylpteridine (20). This compound was prepared via ester **65** by the same method as **19** except that benzyl 5-pentynoate was used and the ion-exchange step was replaced by silica gel chromatography using 85:15:1 (v/v/v) $CHCl_3$/MeOH/AcOH as the eluent. The product was a dark yellowish-brown solid (36% yield); mp 221 °C (dec) with preliminary darkening; MS calcd *m/e* 464.12 (MH^+), found 464.18. Anal. ($C_{26}H_{21}N_7O_2 \cdot 2.6AcOH \cdot 0.6H_2O$) C, N. H: calcd, 5.22; found, 4.68.

2,4-Diamino-6-[2′-(5-carboxy-1-pentynyl)-5*H*-dibenz[*b*,*f*]azepinyl]methylpteridine (21). This compound was prepared via ester **66** by the same method as **19** except that benzyl 6-hexynoate was used and the product was purified in two stages by ion-exchange chromatography using 1.5% NH_4OH followed by silica gel chromatography using 90:10:1.5 (v/v/v) $CHCl_3$/MeOH/AcOH. The product was a dark yellowish-brown solid (16% yield): mp 205 °C (dec) with preliminary darkening; MS *m/e* calcd 477.19 (MH^+), found 477.15. Anal. ($C_{27}H_{23}N_7O_2 \cdot 1.9AcOH \cdot 0.5H_2O$) C, H, N.

2,4-Diamino-5-[3′-(4-carboxy-1-butynyl)-4′-bromo-5′-methoxybenzyl]pyrimidine (22). Step 1. A suspension of **67** (975 mg, 3 mmol)[18] in dry THF (25 mL) was treated with di-*tert*-butyl pyrocarbonate (5.45 g, 25 mmol), Et_3N (840 μL, 606 mg, 6 mmol), and DMAP (60 mg, 0.6 mmol), and the mixture was stirred at room temperature for 20 h. The volatiles were removed by rotary evaporation, and the product was chromatographed twice on silica gel (20−25 g, 2:1 hexanes/EtOAc) to obtain **68** as a gum (1.67 g, 67%) which was then taken up in 10 mL of a 4:1 (v/v) mixture of CH_2Cl_2 and morpholine. The solution was left at room temperature for 3 h, and an additional amount of CH_2Cl_2 was added to allow all of the morpholine to be removed by washing with dilute citric acid until the pH of the aqueous phase was acidic. TLC (silica gel, 1:1 EtOAc/hexanes) showed a major spot with a R_f value of 0.5 and two minor spots with R_f values of 0.4 and 0.3. Chromatography on flash-grade silica gel (50 g, 3 cm × 19 cm) using 1:1 EtOAc/hexanes gave the phenol **69** as a soft solid (772 mg, 53%). The minor impurities with R_f values of 0.4 and 0.3 eluted more slowly and appeared from ^1H NMR spectra to contain less than four *N*-Boc groups. The entire batch of **69** (772 mg, 1.06 mmol) was dissolved in pyridine (5 mL), and the solution was cooled in an ice bath, treated with triflic anhydride (673 μL, 1.13 mg, 4 mmol), and placed in the refrigerator at 4 °C for 20 h. The reaction mixture was then diluted with CH_2Cl_2 and washed with dilute citric acid until all the pyridine was removed. Evaporation under reduced pressure followed by flash chromatography (silica gel, 15 g, 2 cm × 13 cm) afforded the triflate **70** as a soft solid (812 mg, 95%); ^1H NMR ($CDCl_3$) δ 1.32 (s, 18H, $N(Boc)_2$), 1.37 (s, 18H, $N(Boc)_2$), 3.82 (s, 5H, bridge CH_2 and OMe), 6.67 (s, 1H, aryl H), 6.72 (s, 1H, aryl H), 8.50 (s, 1H, pyridine H_5). The entire batch of **70** (812 mg, 0.95 mmol) was combined with benzyl 4-butynoate (338 mg, 1.8 mmol) in a mixture of DMF (3 mL) and Et_3N (3 mL), and the solution was stirred under N_2, treated with 100 mg each of $(Ph_3P)_3CuBr$ and of $(Ph_3P)_2PdCl_2$, and heated at 55 °C for 20 h. The volatiles were removed by rotary evaporation, and the residue was taken up in 30 mL of 2:1 CH_2Cl_2/TFA to remove the Boc groups. After 1 h at room temperature, the solution was concentrated to dryness, the residue was taken up in DMSO (5 mL), and 2 N NaOH (15 mL) was added with swirling. A precipitate formed, suggesting incomplete saponification. Additional H_2O (60 mL) was added, the supernatant was decanted, and the undissolved solid was treated again with NaOH in DMSO as above. A small amount of solid still failed to dissolve and was filtered off. The filtrate was frozen and thawed, a final trace of undissolved material was removed, and all of the solutions containing the product were adjusted to pH 9 with 10% AcOH. Preparative HPLC (C_{18} silica gel, 15% MeCN in 0.1 M NH_4OAc, pH 7.4) yielded a major peak, and a number of minor peaks which were discarded. The major peak was collected and freeze dried, and the residue was purified further on a column of DEAE-cellulose (20 g, 1.5 cm × 22 cm, HCO_3^- form). The column was initially eluted with H_2O, then 0.4 M NH_4HCO_3, and finally 0.4 M NH_4HCO_3 adjusted to pH 10 with 28% NH_4OH. Eluates were monitored by HPLC, pooled appropriately, and freeze dried to obtain **22** as a white solid (83 mg, 20% based on **70**): mp >250 °C (dec); MS calcd *m/e* 405.06, 407.06 (MH^+) for the two stable Br isotopes; found 405.11, 407.11. Anal. ($C_{17}H_{17}BrN_4O_3 \cdot 2H_2O$) C, H, N.

2,4-Diamino-5-methyl-6-[2′-methoxy-5′-(3-carbethoxypropyl)oxybenzyl]pyrido-[2,3-*d*]pyrimidine (30). Metallic Na (29.9 mg, 1.3 mmol) was dissolved in absolute EtOH (2 mL), the solvent was evaporated under reduced pressure, the residue of NaOEt was taken up in anhydrous DMSO (2 mL), and the mixture was stirred at room temperature for 30 min. Crude **29** (4.36 g, 10 mmol; cf. Supporting Information) and ethyl 4-bromobutanoate (254 mg, 1.3 mmol) were then added, the reaction mixture was kept at room temperature overnight, and H_2O was added until a copious precipitate formed. The product was extracted several times with $CHCl_3$, the combined extracts were evaporated, and the solid was purified by flash chromatography (silica gel, 9:1 $CHCl_3$/MeOH) followed by recrystallization from EtOH to obtain ester **30** as a beige solid (90 mg, 17%): mp 226−227 °C; MS calcd *m/e* 426.21 (MH^+), found 426.28. Anal. ($C_{22}H_{27}N_5O_4$) C, H, N.

2,4-Diamino-5-methyl-6-[2′-methoxy-5′-(4-carbethoxybutyl)oxybenzyl]pyrido-[2,3-*d*]pyrimidine (31). This compound was obtained in 17% yield from crude **29** by the same method as ester **30**: mp 215−216 °C; MS calcd *m/e* 440.23 (MH^+), found 440.37. Anal. ($C_{23}H_{29}N_5O_4 \cdot 1.4H_2O$) C, H, N.

2,4-Diamino-5-methyl-6-[2′-methoxy-5′-(5-carbethoxypentyl)oxybenzyl]pyrido-[2,3-*d*]pyrimidine (32). This compound was obtained in 15% yield from crude **29** by the same method as ester **30**: mp 226−227 °C; MS calcd *m/e* 454.25 (MH^+), found 454.23. Anal. ($C_{24}H_{31}N_5O_4 \cdot 0.35H_2O$) C, H, N.

(*Z*/*E*)-4-Chloro-2-[(2-benzyloxy-5-methoxy)benzyl]-3-propen-2-one (35a/35b). Phosphorus oxychloride (18.6 mL, 31 g, 0.2 mol) was added dropwise with stirring into DMF (20 mL) at 0 °C. An off-white suspension formed initially and redissolved upon warming to room temperature. The resulting amber-colored solution of Vilsmeier reagent was treated with a solution of **34** (28.4 g, 0.1 mol) in DMF (20 mL), and the mixture was stirred at room temperature for 1 h and treated first with crushed ice and then carefully with 20% $NaHCO_3$ until no more effervescence occurred. The resulting solution was extracted several times with Et_2O, and the pooled organic layers were dried and evaporated to a greenish oil whose TLC showed the presence of two spots. Although these two products could be separated by silica gel chromatography and were able to be identified as **35a** and **35b**, the reaction with cyanoacet-

amide in the next step was carried out using the *E*/*Z* mixture. **35a** (*Z*-isomer): white solid (2.91 g, 18%); mp 53−54 °C. Anal. ($C_{19}H_{19}ClO_3$) C, H, Cl. **35b** (*E*-isomer): pale-green oil (6.80 g, 41%). Anal. ($C_{19}H_{19}ClO_3$) C, H, Cl.

5-[(2′-Benzyloxy-5′-methoxy)benzyl]-3-cyano-4-methyl-2-pyridone (36). Sodium hydride (3.45 g, 60% dispersion in mineral oil, 0.086 mol) was added in small portions to a solution of cyanoacetamide (7.24 g, 0.086 mol) in dry THF (500 mL), and the white suspension was stirred at room temperature for 1 h. The mixture was then cooled to −15 °C and treated dropwise with a solution of **35a/35b** (9.50 g, 0.029 mol) in THF (150 mL). The mixture was slowly warmed to room temperature and refluxed for 1 h. The resulting yellow suspension was then cooled and treated with H_2O, and the mixture was concentrated to dryness under vacuum. The residue was purified extensively (3 times) by flash chromatography on silica gel (97:3 $CHCl_3$/MeOH), with individual fractions of the eluent being monitored by TLC with the same mixture of solvents. Fractions showing a single spot (R_f 0.1) were pooled and evaporated to obtain **36** as a white solid (4.62 g, 45%): mp 218−220 °C. Anal. ($C_{22}H_{20}N_2O_3$) C, H, N.

A second faster-moving compound (2.60 g, 25% R_f 0.19) was also isolated from the column and discarded. While the elemental analysis on this material was not obtained, its ^{1}H NMR spectrum suggested that it was probably the unwanted regioisomer 5-[(2′-benzyloxy-5′-methoxy)benzyl]-3-cyano-6-methyl-2-pyridone (**36a**, cf. Scheme 2): ^{1}H NMR (DMSO-d_6) δ 2.17 (s, 3H, 6-CH_3), 3.60 (s, 3H, OMe), 3.78 (s, 2H, bridge CH_2), 5.05 (s, 2H, OCH_2Ph), 6.34 (d, 1H, J = 2.9 Hz, H_3), 6.68 (dd, 1H, J = 2.9 Hz, 9.2 Hz, $H_{4'}$), 6.94 (d, 1H, J = 9.2 Hz, $H_{3'}$), 7.04−7.40 (m, 5H, aryl H), 7.69 (s, 1H, pyridone H_4), 7.86 (br s, lactam NH). Because of the extreme difficulty of eliminating this impurity, further use of **36** as an intermediate to 2′-O-substituted PTX analogues was abandoned except for its conversion to **38** via **37** as detailed below.

2-Chloro-5-[(2′-benzyloxy-5′-methoxy)benzyl]-3-cyano-4-methylpyridine (37). Oxalyl chloride (7.8 g, 61.5 mmol) was added dropwise to $CHCl_3$ (25 mL) and DMF (4.68 g, 64 mmol) at 0 °C, and the colorless solution was warmed to room temperature and stirred for 3 h. Compound **36** (2.16 g, 6 mmol) was then added, and the mixture was refluxed for 3 h before being cooled back to room temperature, chilled to 0 °C, and treated slowly with n-$BuNH_2$ (30 mL) over a period of 1 h and under reflux for another 30 min. The solvents were evaporated under vacuum, and the dark-brown residue was chromatographed twice on flash silica gel using 9:1 cyclohexanes/EtOAc and then 99:1 CH_2Cl_2/EtOAc as the eluents. Evaporation of appropriately pooled fractions yielded a white solid (0.73 g, 32%). Recrystallization of a portion of this solid from EtOH gave **37** as fine white needles: mp 101−102 °C. Anal. ($C_{22}N_{19}$-ClN_2O_2) C, H, N, Cl.

2,4-Diamino-5-methyl-6-(2′-benzyloxy-5′-methoxybenzyl)pyrido[2,3-*d*]pyrimidine (38). Metallic Na (104 mg, 4.6 mmol) was dissolved in MeOH (10 mL), the solution was cooled in an ice bath, and guanidine hydrochloride (500 mg, 5.2 mmol) was added. The mixture was stirred for 15 min, the fine white precipitate was suction filtered, and the filtrated was evaporated to dryness. A solution of **37** (250 mg, 0.66 mmol) in anhydrous pyridine (1.5 mL) was added. The solution was kept at 70 °C for 1.5 h and heated to reflux for 4 h. After being cooled to room temperature, the solution was diluted with H_2O and kept at 0 °C until a precipitate formed, which was filtered, dried under vacuum, and purified by silica gel flash chromatography (95:5 $CHCl_3$/MeOH) to obtain **38** as a white solid (49 mg, 18%): mp 259−261 °C; MS calcd *m*/*e* 402.19 (MH^+), found 402.08. Anal. ($C_{23}H_{23}N_5O_2 \cdot 0.25H_2O$). C, H, N.

2,4-Diamino-5-methyl-6-[2′-(carbethoxypropyloxy)-5′-methoxybenzyl]pyrido[2,3-*d*]pyrimidine (45). Step 1. A mixture of **41** (41.8 g, 0.117 mol; cf. Supporting Information) and 2,4,6-triaminopyrimidine (14.7 g, 0.117 mol) in NMP (100 mL) was heated at 190 °C in a two-neck round-bottom flask fitted with a Dean−Stark trap for 3 h. The dark-amber solution was cooled to room temperature until a beige-colored solid formed. After the addition of MeOH (180 mL), the product was collected by suction filtration and the filter cake washed with boiling H_2O to obtain **42** as a solid pure enough to be used in the next step without additional purification. The solid was initially colorless but turned yellow upon being dried in vacuo at room temperature over P_2O_5; MS calcd *m*/*e* 418.19 (MH^+), found 418.05.

Step 2. Oxalyl chloride (21.5 mL, 31.7 g, 0.25 mol) was added dropwise to a stirred solution of DMF (19.6 g, 20.8 mL, 0.27 mol) in CH_2Cl_2 (120 mL) at 0 °C. When addition was complete, the mixture was brought back to room temperature and stirred for 15 h. Compound **42** (10.4 g, 0.025 mol) was then added, and the mixture was refluxed for 3 h, chilled to 0 °C, and treated slowly with n-$BuNH_2$ (60 mL) during 2 h followed by another 1.5 h of reflux. The reaction mixture was cooled to room temperature, the volatiles were removed by rotary evaporation, and the black residue was triturated with a mixture of crushed ice and H_2O until a beige solid formed, which was dried in vacuo over P_2O_5 and partially purified by silica gel flash chromatography (9:1 $CHCl_3$/MeOH, R_f 0.37). The resulting chloride **43** (2.6 g, 25%) was used in the next step without further purification; MS calcd *m*/*e* 436.15 (MH^+), found 436.01.

Step 3. A mixture of partly purified **43** (7.76 g, 17.8 mmol) and 5% Pd−C (3.6 g) in 2-methoxyethanol (200 mL) was refluxed while slowly adding sodium formate (7.3 g, 107 mmol) over a period of 4 h. The mixture was filtered through a Celite pad, the filtrate was evaporated under reduced pressure, the dark residue was taken up directly in DMSO (20 mL), and the solution was added to ethanolic NaOEt prepared from 62.5 mg of metallic Na and EtOH (2 mL). The resulting dark-brown solution, assumed to contain the Na salt of **44**, was treated dropwise with ethyl 4-bromobutanoate (0.389 mL, 530 mg, 2.72 mmol) and stirred at room temperature overnight. After the addition of H_2O (100 mL), the product was extracted with $CHCl_3$ (2 times), the pooled extracts were evaporated, and the residue was purified by silica gel chromatography (9:1 $CHCl_3$/MeOH) and recrystallization from 95% EtOH to obtain **45** as yellow needles (240 mg, 21%): mp 224−226 °C; MS calcd *m*/*e* 426.21 (MH^+), found 426.15. Anal. ($C_{22}H_{27}N_5O_4 \cdot 0.35H_2O$) C, H, N.

Molecular Modeling. Unrestrained dynamics simulations using the program AMBER 7[26] were of 1-ns duration and were performed with slight modifications as described earlier.[8]

Acknowledgment. This work was supported by research Grant RO1-AI29904 (to A.R.) from the National Institute of Allergy and Infectious Diseases, National Institutes of Health, and Department of Health and Human Services. We are grateful to the help of Dr. Joel E. Wright and Dr. Ying-Nan Chen in performing the cell growth inhibition assays.

Supporting Information Available: Elemental analyses for all of the new compounds. Detailed synthetic procedures and physical constants for benzyl 4-pentynoate, benzyl 5-hexynoate, benzyl 5-heptynoate, and intermediates **24**−**29**, **34**, **37**−**39**, and **47**−**53**, IR data for compounds **6**−**14**, **19**−**22**, **26**, **30**−**32**, **34**, **36**−**41**, **41**, **45**, **48**, **53**, **55**, and **56**. ^{1}H NMR data for compounds **6**−**14**, **19**−**22**, **25**, **26**, **30**−**32**, **34**−**43**, **45**, **48**, **51**−**57**, and **63**. This material is available free of charge via the Internet at http://pubs.acs.org.

References

(1) *Pneumocystis carinii* is now also known as *Pneumocystis jiroveci*, but this nomenclature change has been somewhat controversial. For two divergent views on the subject, see: (a) Hughes, W. T. *Pneumocystis carinii* vs *Pneumocystis jiroveci*: another misnomer (response to Stringer et al.). *Emerging Infect. Dis.* **2003**, *9*, 276−277. (b) Stringer, J. R.; Beard, C. B.; Miller, R. F.; Cushion, M. T. A new name (*Pneumocystis jiroveci*) for Pneumocystis from humans (response to Hughes), *Emerging Infect. Dis.* **2003**, *9*, 277−279. Because the name *Pneumocystis carinii* was used in all of our previous papers reporting the inhibition of DHFR from organisms isolated from immunosuppressed rats, we will retain this name in the present paper.

(2) Rosowsky, A.; Forsch, R. A.; Queener, S. F. Inhibition of *Pneumocystis carinii*, *Toxoplasma gondii*, and *Mycobacterium avium* dihydrofolate reductases by 2,4-diamino-5-[2-methoxy-5-(ω-carboxyalkoxy)benzyl]pyrimidines marked improvement in potency relative to trimethoprim and species selectivity relative to piritrexim. *J. Med. Chem.* **2002**, *45*, 233−241.

(3) Rosowsky, A.; Forsch, R. A.; Queener, S. F. Further studies on 2,4-diamino-5- (2′,5′-disubstituted benzyl)pyrimidines as potent and selective inhibitors of dihydrofolate reductases from three major opportunistic pathogens of AIDS. *J. Med. Chem.* **2003**, *46*, 1726−1736.

(4) Forsch, R. A.; Queener, S. F.; Rosowsky, A. Preliminary in vitro studies on two potent, water-soluble trimethoprim analogues with exceptional species selectivity against dihydrofolate reductase from *Pneumocystis carinii* and *Mycobacterium avium*. *Bioorg. Med. Chem. Lett.* **2004**, *14*, 1811−1815, 2693.

(5) Medina, I.; Mills, J.; Leoung, G.; Hopewell, P. C.; Lee, B.; Modin, G.; Benowitz, N.; Wofsy, C. B. Oral therapy for *Pneumocystis carinii* pneumonia in the acquired immunodeficiency syndrome. A controlled trial of trimethoprim-sulfamethoxazole versus trimethoprim-dapsone. *N. Engl. J. Med.* **1990**, *323*, 776−782.

(6) Roudier, C.; Caumes, E.; Rogeaux, O.; Bricaire, F.; Gentilini, M. Adverse cutaneous reactions to trimethoprim-sulfamethoxazole in patients with acquired immunodeficiency syndrome and *Pneumocystis carinii* pneumonia. *Arch. Dermatol.* **1994**, *30*, 1383−1386.

(7) Falloon, J.; Allegra, C. J.; Kovacs, J.; O'Neill, D.; Ogata-Arakaki, D.; Feuerstein, I.; Polis, M.; Davey, R.; Lane, H. C.; LaFon, S.; Rogers, M.; Zunich, K.; Turlo, J.; Tuazon, C.; Parenti, D.; Simon, G.; Masur, H. Piritrexim with leucovorin for the treatment of pneumocystis pneumonia (PCP) in AIDS patients. *Clin. Res.* **1990**, *38*, 361A.

(8) Rosowsky, A.; Fu, H.; Chan, D. C. M.; Queener, S. F. Synthesis of 2,4-diamino-6- [2′-*O*-(ω-carboxyalkyl)oxydibenz[*b*,*f*]azepin-5-yl]methylpteridines as potent and selective inhibitors of *Pneumocystis carinii*, *Toxoplasma gondii*, and *Mycobacterium avium* dihydrofolate reductase. *J. Med. Chem.* **2004**, *47*, 2475−2485.

(9) Periti, O. Brodimoprim, a new bacterial dihydrofolate reductase inhibitor. *J. Chemother.* **1995**, *7*, 221−223.

(10) Then, R. L. Antimicrobial dihydrofolate reductase inhibitors - - achievements and future options. *J. Chemother.* **2004**, *16*, 3−12.

(11) (a) Grivsky, E. M.; Lee, S.; Siegel, C. W.; Duch, D. S.; Nichol, C. A. 2,4-Diamino-6-(2,5-dimethoxybenzyl)-5-methylpyrido[2,3-*d*]-pyrimidine. *J. Med. Chem.* **1980**, *23*, 327−329. (b) Rauckman, B. S.; Woolley, J. L., Jr.; Roth, B. Pyridopyrimidines methods for their preparation and pharmaceutical formulations thereof. EP 0278686; Wellcome Foundation, Ltd., 1988.

(12) It may be noted that numerous piritrexim analogues other than those reported here were described in 1993, but unfortunately the paper appeared in a Chinese language journal which is not readily available in the U.S.; cf.: Zhang, Y.; Zhou, J.; Li, R.; Wu, J.; Zhang, H. Synthesis and studies on the antitumor activities of 2,4-diamino-6-substituted benzyl-5-methylpyrido[2,3-*d*]pyrimidine derivatives. *Chin. J. Med. Chem.* **1993**, *3*, 85−96. From the general synthetic scheme shown in this paper, it appears that the β-keto ester route[11a,b] was the one that these authors used.

(13) Troschütz, R.; Zink, M.; Gnibl, R. An alternative synthesis of piritrexim, a lipophilic inhibitor of human dihydrofolate reductase. *J. Heterocycl. Chem.* **1999**, *36*, 703−706.

(14) Two other approaches that could have been used to obtain potential precursors to compounds **6**−**9** were not pursued. The first, based on work by Hill and co-workers,[15] would involve consecutive reactions of an appropriately 2,5-disubstituted 4-arylbutan-2-one with malononitrile, diethoxymethyl acetate, hydrogen bromide, and guanidine. The second, based on a new regioselective synthesis of PTX recently developed in our own laboratory,[16] would involve Pd(0)-catalyzed coupling between 2-amino-5-bromo- or 2-amino-5-iodonicotinonitrile and a 2,5-disubstituted benzylzinc halide, followed by reaction with $SbBr_3$/*t*-BuONO and then guanidine.

(15) Hill, J. A.; Wisowaty, J. C.; Darnofall, M. E. Synthesis of carbon-14 labeled piritrexim − a potential anticancer agent. *J. Labelled Compd. Radiopharm.* **1993**, *33*, 1119−1130.

(16) Chan, D. C. M.; Rosowsky, A. Synthesis of the lipophilic antifolate piritrexim via a palladium(0)-catalyzed cross-coupling reaction. *J. Org. Chem.* **2005**, *70* (*4*), 1364−1368.

(17) Sonogashira, K.; Tohda, Y.; Hagihara, B. A convenient synthesis of acetylenes. Catalytic substitutions of acetylenic hydrogen with bromo alkenes, iodo arenes, and bromopyridines. *Tetrahedron Lett.* **1975**, *16*, 4467−4470.

(18) For the synthesis of brodimoprim analogues with ω-carboxyalkoxy side chains (as opposed to a ω-carboxy-1-alkynyl) side chain from this key intermediate, see: Kompis, I.; Then, R. L. Rationally designed brodimoprim analogues: synthesis and biological activities. *Eur. J. Med. Chem.* **1984**, *19*, 529−534.

(19) Rosowsky, A.; Cody, V.; Galitsky, N.; Fu, H.; Papoulis, A. T.; Queener, S. F. Structure-based design of selective inhibitors of dihydrofolate reductase: synthesis and antiparasitic activity of 2,4-diaminopteridine analogues with a bridged diarylamine side chain. *J. Med. Chem.* **1999**, *42*, 4853−4860.

(20) Gangjee, A.; Adair, O.; Queener, S. F. *Pneumocystis carinii* and *Toxoplasma gondii* dihydrofolate reductase inhibitors and antitumor agents: synthesis and biological activities of 2,4-diamino-5-methyl-6-[(monosubstituted anilino)methyl]pyrido-[2,3-*d*]pyrimidines. *J. Med. Chem.* **1999**, *42*, 2447−2455.

(21) Wright, J. E.; Vaidya, C. M.; Chen, Y.-N.; Rosowsky, A. Efficient utilization of the reduced folate carrier in CCRF−CEM human leukemic lymphoblasts by the potent antifolate N^{α}-(4-amino-4-deoxypteroyl)-N^{δ}-hemiphthaloyl-L-ornithine (PT523) and its B-ring analogues. *Biochem. Pharmacol.* **2000**, *60*, 41−46.

(22) Champness, J. N.; Achari, A.; Ballantine, S. P.; Bryant, P. K.; Delves, C. J.; Stammers, D. K. The structure of *Pneumocystis carinii* dihydrofolate reductase to 1.9 Å resolution. *Structure* **1994**, *2*, 915−924.

(23) Stammers, D. K.; Delves, C.; Ballantine, S.; Jones, E. Y.; Stuart, D. I., Achari, A. Bryant, P. K.; Champness, J. N. Preliminary crystallographic data for *Pneumocystis carinii* dihydrofolate reductase. *J. Mol. Biol.* **1993**, *230*, 679−680.

(24) Oefner, C.; D'Arcy, A.; Winkler, F. K. Crystal structure of human dihydrofolate reductase complexes with folate. *Eur. J. Biochem.* **1988**, *174*, 377−385.

(25) Nahimana, A.; Rabodonirina, M.; Bille, J.; Francioli, P.; Hauser, P. M. Mutations of *Pneumocystis jirovecii* dihydrofolate reductase associated with failure of prophylaxis. *Antimicrob. Agents Chemother.* **2004**, *48*, 4301−4305. As noted in this paper, a newly identified problem associated with antifolate prophylaxis of pneumocystis pneumonia in immunocompromised populations is the emergence of drug-resistant DHFR in the face of selection pressure with lipophilic inhibitors such as pyrimethamine. The name *Pneumocystis jirovecii* has also been used instead of the earlier version, *Pneumocystis jiroveci*; cf. Nahimana, A.; Rabodonirina, A.; Zanetti, G.; Meneau, I.; Francioli, P.; Bille, J.; Hauser, P. M. Association between a specific *Pneumocystis jirovecii* dihydropteroate synthase mutation and failure of pyrimethamine prophylaxis in human immunodeficiency virus-positive and -negative patients. *J. Infect. Dis.* **2003**, *188*, 1017−1023.

(26) Case, D. A.; Pearlman, D. A.; Caldwell, J. W.; Cheatham, T. E. III; Wang, J.; Ross, W. S.; Simmerling, C. L.; Darden, T. A.; Merz, K. M.; Stanton, R. V.; Cheng, A. L.; Vincent, J. J.; Crowley, M.; Tsui, V.; Gohlke, H.; Radmer, R. J.; Duan, Y.; Pitera, J.; Massova, I.; Seibel, G. L.; Singh, U. C.; Weiner, P. K.; Kollman, P. A. *AMBER 7*; University of California: San Francisco, CA, 2002.

JM0581718